



**HAL**  
open science

## Links between sediment structures and ecological processes in the hyporheic zone: ground-penetrating radar as a non-invasive tool to detect subsurface biologically active zones

Florian Mermillod-Blondin, Thierry Winiarski, Arnaud Foulquier, Anne Perrissin, Pierre Marmonier

### ► To cite this version:

Florian Mermillod-Blondin, Thierry Winiarski, Arnaud Foulquier, Anne Perrissin, Pierre Marmonier. Links between sediment structures and ecological processes in the hyporheic zone: ground-penetrating radar as a non-invasive tool to detect subsurface biologically active zones. *Ecohydrology*, 2015, 8 (4), pp.626-641. 10.1002/eco.1530 . hal-01323969

**HAL Id: hal-01323969**

**<https://sde.hal.science/hal-01323969>**

Submitted on 15 Sep 2023

**HAL** is a multi-disciplinary open access archive for the deposit and dissemination of scientific research documents, whether they are published or not. The documents may come from teaching and research institutions in France or abroad, or from public or private research centers.

L'archive ouverte pluridisciplinaire **HAL**, est destinée au dépôt et à la diffusion de documents scientifiques de niveau recherche, publiés ou non, émanant des établissements d'enseignement et de recherche français ou étrangers, des laboratoires publics ou privés.

# Links between sediment structures and ecological processes in the hyporheic zone: ground-penetrating radar as a non-invasive tool to detect subsurface biologically active zones

Florian Mermillod-Blondin,<sup>1\*</sup> Thierry Winiarski,<sup>1</sup> Arnaud Foulquier,<sup>2</sup> Anne Perrissin<sup>3</sup>  
and Pierre Marmonier<sup>1</sup>

<sup>1</sup> UMR5023 Ecologie des Hydrosystèmes Naturels et Anthropisés, Université de Lyon, Université Lyon 1, ENTPE, CNRS, 6 rue Raphaël Dubois, 69622 Villeurbanne, France

<sup>2</sup> Irstea, Groupement de Lyon, UR MALY, 5 Rue de la Doua, 69626 Villeurbanne, France

<sup>3</sup> Grand Lyon, Direction de l'Eau, 20, rue du Lac, 69399 Lyon, France

## ABSTRACT

At the scale of geomorphological units (riffles, pools, and gravel bars), the contribution of the hyporheic zone to the functioning of streams and rivers depends on the hydrological exchanges between surface water and groundwater. These exchanges are largely controlled by sediment structure and texture, which are difficult to assess with classical methods (shovelling and freeze coring). We aimed to evaluate the ability of a non-destructive method, ground-penetrating radar (GPR), to detect sediment structures associated with subsurface biologically active zones in a gravel-bed river. After GPR data acquisition and processing, a three-dimensional reconstruction of a gravel bar permitted the identification of two sediment facies: a cobble/gravel lithofacies denoted as 'coarse' and a sand/gravel lithofacies denoted as 'fine'. We installed piezometers along two longitudinal profiles (each corresponding to a lithofacies identified by GPR) and monitored hydraulic head and temperature for 20 days. Water and sediments were sampled along the two profiles to measure water physicochemistry, sediment characteristics, bacterial abundance and activity, and interstitial invertebrate assemblages. These measurements confirmed that the two profiles were characterized by distinct hydrological flow rates and associated biological activities. Rapid water transport in the coarse profile fuelled the hyporheic zone with organic matter, whereas water and organic matter supplies were lower in the fine profile. Consequently, the higher supply of organic matter in the coarse profile was associated with higher microbial activities and invertebrate density and diversity. Therefore, GPR could be an efficient tool to detect the sediment features playing a key role in hyporheic zone functioning.

KEY WORDS gravel bar; hyporheic hotspots; geophysics; lithofacies; hydrological processes; hyporheic fauna; microbial activity;

## INTRODUCTION

The subsurface sediment of streams and rivers (the hyporheic zone, Orghidan, 1959) plays a key role in the hydrology, material cycling, and energy flow of lotic ecosystems (Jones and Holmes, 1996; Brunke and Gonser, 1997; Boulton *et al.*, 1998; Krause *et al.*, 2011). Many important biogeochemical processes have been shown to occur intensively in the hyporheic zone of streams, such as respiration (Pusch, 1996), nitrification (Jones *et al.*, 1995a; Butturini *et al.*, 2000), denitrification (Holmes *et al.*, 1996; Lefebvre *et al.*, 2004; Storey *et al.*, 2004), and

methanogenesis (Jones *et al.*, 1995b). Its significance to hydrosystem function is largely dependent on the hydrological connections and associated organic matter supply between surface and interstitial habitats (Hendricks, 1993; Jones *et al.*, 1995c; Fellows *et al.*, 2001). For instance, Battin (2000) showed that the hydrolytic activity of hyporheic bacterial biofilms was positively linked to hydrological exchanges. Tonina and Buffington (2009) reported the main mechanisms driving hydrological connections between surface and interstitial habitats over multiple spatial scales. At the scale of geomorphological units (riffles, pools, and gravel bars), exchanges between surface water and groundwater are ultimately controlled by hydrology and sediment structure (Vervier *et al.*, 1992; Claret *et al.*, 1998; Battin *et al.*, 2008). Monitoring hydraulic heads has been largely used to determine hydraulic gradients and infer water flows within geomorphological units

\*Correspondence to: Florian Mermillod-Blondin, UMR5023 Ecologie des Hydrosystèmes Naturels et Anthropisés, Université Lyon 1, ENTPE, CNRS, Université de Lyon, 6 rue Raphaël Dubois, 69622 Villeurbanne, France.  
E-mail: mermillo@univ-lyon1.fr

(Bencala and Walters, 1983; Valett *et al.*, 1997; Poole *et al.*, 2006), but valid information about sediment structure and texture is more difficult to obtain because of disturbances associated with shovelling or freeze-coring sampling techniques (Marmonier *et al.*, 2004; Descloux *et al.*, 2010).

Ground-penetrating radar (GPR) is a powerful non-destructive tool for investigating fluvial deposits in detail up to a depth of 20 m (Leclerc and Hickm, 1997; Gourry *et al.*, 2003; Neal, 2004; Mumphy *et al.*, 2007) and is especially effective in coarse-grained (gravel and sand) environments (Best *et al.*, 2003; Heinz *et al.*, 2003; Lunt *et al.*, 2004). GPR allows the documentation of the internal structure (bedding geometry) of active braided bars and channels under both water-saturated and unsaturated conditions (Lunt *et al.*, 2004; Mumphy *et al.*, 2007). It has also been used to estimate water content and porosity within the hyporheic zone (Brosten *et al.*, 2009). This is also the unique geophysical method currently existing for the acquisition of shallow, high-resolution, continuous data (Neal, 2004; Schrott and Sass, 2008). Despite the many opportunities existing for employing this methodology to characterize the sediment habitats of fluvial environments and their expected influences on the distribution of biotic processes (Naegeli *et al.*, 1996), GPR has not yet been used by aquatic ecologists to assess the links between subsurface biological processes and sediment structure within the hyporheic zone.

The present study aimed to fill this gap by evaluating the ability of GPR to detect sediment structures associated with distinct biological processes in the subsurface of a gravel-

bed river. We used high-resolution continuous GPR profiling to obtain the detailed sediment structure of a gravel bar. After data processing and interpretations, two distinct sediment structures were selected along the gravel bar: one dominated by cobbles and gravel (denoted as ‘coarse’) and one rich in sands and gravel (denoted as ‘fine’). According to the literature (Wood and Armitage, 1997; Lefebvre *et al.*, 2005), we expected that a hydrological connection with the surface would be more pronounced within the coarse sediment structure than within the fine sediment structure. Consequently, the coarse sediment structure would be more biologically active in terms of microbial activity and hyporheic fauna than the fine sediment structure.

## MATERIALS AND METHODS

### Study site

The study was carried out in a channel (Vieux Rhône) of the Rhône River located about 2 km upstream from Lyon (France) and upstream from the pumping well field of ‘Crépieux-Charmy’ (Figure 1), which provides drinking water for the Lyon metropolitan area. The bed sediments are made of a coarse substrate mainly composed of cobbles and gravels (Poinsart *et al.*, 1989). We selected a gravel bar located on the right bank of the Vieux Rhône channel. The Vieux Rhône channel is a regulated channel, and its discharge remained constant along most of the experiment duration but decreased by 60 cm on the last day of the experiment.

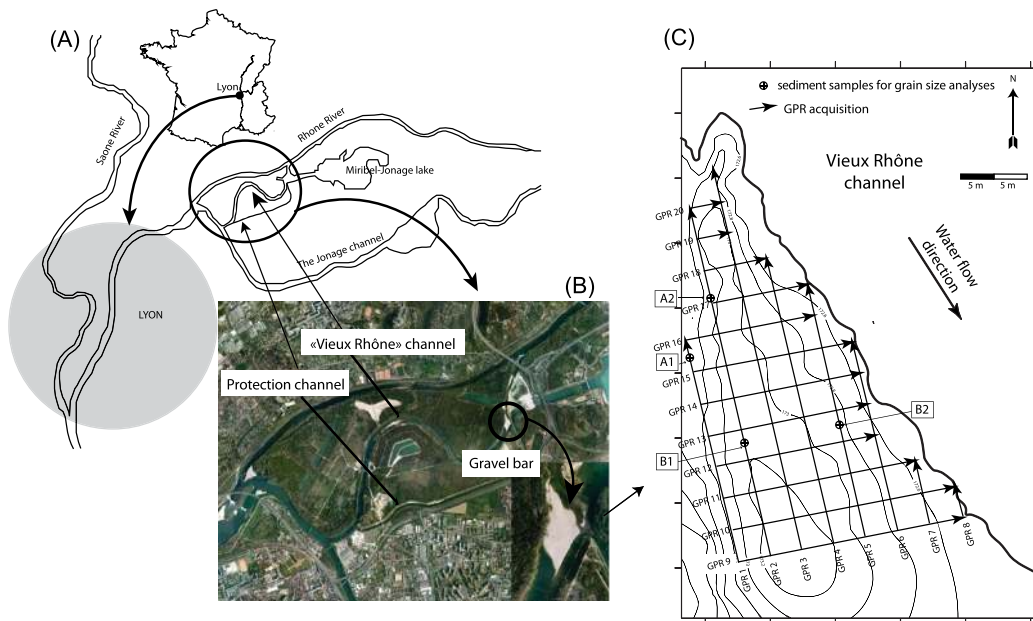


Figure 1. Location of the Rhône River, Lyon, France (A), aerial photograph indicating the location of the studied gravel bar (B), and layout of the 5 m x 5 m rectilinear ground-penetrating radar (GPR) acquisition grid with GPR profile designations (C). Positions of sediment samples for grain size analyses are indicated by A1, A2, B1, and B2.

### *GPR method*

Ground-penetrating radar is a non-invasive geophysical technique that detects electrical discontinuities in the shallow subsurface. This technique is based on the generation, transmission, propagation, reflection, and reception of discrete pulses of high-frequency (MHz) electromagnetic energy. It allows the assessment of spatial structures of sediments to a depth of 10–20 m over extended areas (Huggenberger *et al.*, 1994; Beres *et al.*, 1995; Bridge and Lunt, 2006). Sediment geologists widely used this technique to reconstruct depositional environments and document historic sediment processes (Schrott and Sass, 2008). Indeed, alluvial deposits are characterized by a textural heterogeneity derived from erosion, transport, and sedimentation phases that have led to the current configuration of lithological units. In the present paper, the term lithofacies has been used as a reference to lithological units of fluvial deposits, each lithofacies corresponding to a genetic unit (i.e. formed by a homogeneous process of transport and sedimentation, Miall, 1999).

The GPR measurements were carried out with the GSSI SIR 3000 system (Geophysical Survey System Inc., Salem, USA), operated with a shielded antenna at a central frequency of 400 and 200 MHz, running in monostatic mode. The data processing was performed using the GSSI Radan 6 software. This processing consisted of a distance normalization, a static time shift (to align direct ground wave arrival to 0 ns), a background removal (to eliminate the high-amplitude direct ground wave), and a Kirchhoff migration. The electromagnetic wave velocity was determined by common midpoint with two 400-MHz antennas. This velocity ranged from  $0.12 \text{ m ns}^{-1}$  in the unsaturated zone to  $0.06 \text{ m ns}^{-1}$  in the saturated zone. Accordingly, a velocity of  $0.06 \text{ m ns}^{-1}$  was selected to convert two-way travel time into actual depth, a velocity that is comparable with those measured in the saturated zone of analogous alluvial deposits using the common midpoint method (Woodward *et al.*, 2003; Neal, 2004; Mumphy *et al.*, 2007; Lindhorst *et al.*, 2008). In addition, a topographic survey of the bar using a D-GPS Trimble station was performed to localize the acquisition grid, the topography of the gravel bar, the position of the gravel bar relative to the Vieux Rhône channel, and the position of sediment samples that were used to validate GPR interpretations. Topographic corrections were applied to the data using transect elevation data collected during this survey.

The 400- and 200-MHz profiles were collected in a  $5 \text{ m} \times 5 \text{ m}$  grid pattern (Figure 1C) positioned in the north of the gravel bar. The dimensions of the acquisition grid were  $60 \text{ m} \times 40 \text{ m}$ , and the grid was oriented  $350^\circ \text{N}$ , parallel to the Vieux Rhône channel. The spacing between each grid line was set at 5 m. GPR measurements (400 and 200 MHz) were performed on all acquisition grid lines.

The GPR data set was interpreted using radar facies analysis (Regli *et al.*, 2002; Jol and Bristow, 2003; Mumphy *et al.*, 2007; Bridge, 2009) in conjunction with the classification of seismic reflections developed by Mitchum *et al.* (1977). During interpretation of the profiles, constant gain was applied to the data to note the amplitude of reflections. The GPR profiles were exported into an image file format (.bmp), and major reflections were traced out and coloured using Illustrator CS6 drafting software (Adobe, Inc.). The radar facies packages were positioned in a three-dimensional (3D) context to view spatial relationships between profiles using RockWorks16 geological software (RockWare, Inc.). As GPR profiles acquired an immense amount of interpreted sedimentological information, only major radar reflection packages were described with the profiles of 200-MHz antennae. The profiles of 400-MHz antennae (not presented in this paper) were used to confirm the interpretation of profiles obtained with the 200-MHz antennae.

To validate the interpretation of GPR results, grain size analyses (NF P94-056 standard, Association Française de Normalisation, 1996) were performed on four samples collected at the surface of the gravel bar (Figure 1C). Briefly, around 51 g of sediment was collected per sampled point, dried, and sieved on a set of sieves with mesh sizes varying from 0.1 to 50 mm. The dry sediment was weighted for each retained size fraction and reported as a percentage of the total dry mass of the sediment sample.

### *Sampling procedure*

Following the 3D GPR interpretations, two longitudinal profiles of the bar were selected: one profile with a sediment structure dominated by cobbles and gravel (denoted as coarse) and a second profile associated with sand and gravel (denoted as fine). For each longitudinal profile, three positions were selected at increasing distances from the Vieux Rhône channel along the flow path: 1, 15, and 35 m. For each of these three positions, a pipe (30-mm internal diameter, with holes of 5-mm diameter around the base) was inserted into the bar sediments to reach a depth of 30 cm below the water table. These pipes ( $n=6$ , 3 positions within the gravel bar  $\times$  2 sediment structures) were equipped with probes (Mini-Diver, Schlumberger Water Services, Waterloo, Canada) to monitor pressure and temperature dynamics during the experiment (from 20 May to 9 June 2011). They were closed with caps to prevent any contamination from the surface. At the end of the monitoring period (9 June 2011), three replicate samples of water and sediments were collected using a mobile pipe at each position (1, 15, or 35 m) in the two sediment structures to measure water physicochemistry (pH, electrical conductivity, dissolved oxygen, dissolved organic carbon, nitrate, ammonium, and phosphate concentrations),

characteristics of collected sediments (grain size distribution, total nitrogen, and total organic carbon), bacterial abundance and activity (respiration and hydrolytic activity), and interstitial invertebrate assemblages. At each position, the three replicate samples were spaced about 1.5 m apart to form an equilateral triangle around the pipe equipped with probes. These replicate samples allowed comparisons between sediment structures (coarse structure vs fine structure) along the flow paths. We also collected surface water at three points in the Vieux Rhône channel upstream of the gravel bar.

#### *Sampling technique*

Water and sediment were collected using the Bou–Rouch method (Bou and Rouch, 1967; Bou, 1974). A mobile steel standpipe (25 mm in internal diameter, openings of 5 mm) was inserted to a depth of 30 cm below the water table. Interstitial water was sampled with a syringe to measure electrical conductivity (LF92, WTWTM, Weilheim, Germany), pH, and dissolved oxygen ( $O_2$ ) concentration (HQ20, HACHTM, Dusseldorf, Germany). Afterwards, 10 l of interstitial water mixed with fine sediment was extracted using a hand pump and collected in a plastic box, pre-washed with acid and deionized water, for chemical (in interstitial water and sediments) and bacterial (on sediments) measurements. From each sample, 50 ml of water was filtered through 0.7- $\mu\text{m}$ -pore-size Whatman GF/F filters (Millipore, Billerica, MA, USA) for subsequent analyses of nitrate, ammonium, and phosphate, and 25 ml of water was filtered through a 0.45- $\mu\text{m}$ -pore-size Millipore HAWP filters (Millipore, Billerica, MA, USA) for subsequent analyses of dissolved organic carbon. The same procedure was followed for surface water samples collected from the Vieux Rhône channel. After collection of water samples, the remaining mix of interstitial water and sediment was elutriated three times to separate interstitial fauna from the denser sediment particles. As the Vieux Rhône channel was large and not surrounded by dense riparian vegetation, we did not collect significant proportions of leaf litter debris in hyporheic samples, and most of the particulate organic matter collected was associated with sediments. During elutriation, interstitial fauna was collected using a 200- $\mu\text{m}$ -mesh net and preserved with 96% ethanol. The remaining sediment was collected in a sterile glass vial for physicochemical and microbial analyses. Water and sediment samples were kept in an isotherm box during the 30-min journey back to the laboratory.

#### *Water analyses for nutrients and dissolved organic carbon*

$\text{NH}_4^+$ ,  $\text{NO}_x$ , ( $\text{NO}_3^- + \text{NO}_2^-$ ), and  $\text{PO}_4^{3-}$  concentrations were measured on water samples filtered in the field following standard colorimetric methods (Grasshoff *et al.*, 1983) using a sequential automatic analyser (Easychem Plus, Systea, Anagni, Italy). The concentration of dissolved

organic carbon in filtered water samples was measured with a total carbon analyser (multi-N/C 3100, Analytik Jena, Jena, Germany) based on combustion at 900 °C after removal of dissolved inorganic C with HCl and  $\text{CO}_2$  stripping under  $O_2$  flow.

#### *Sediment analyses*

Each sediment sample was wet-sieved at 1600  $\mu\text{m}$  to perform grain size distribution analyses and total organic carbon, total nitrogen, and microbial measurements on particles with sizes lower than 1600  $\mu\text{m}$ . This procedure was chosen to homogenize sediment particle sizes in order to reduce the potential influence of grain size distribution on microbial activities (as observed in hyporheic sediments by Rulík and Spáčil, 2004).

Grain size volumic proportions of sediment samples were measured by laser diffractometry (Malvern Mastersizer 2000G) on particles ranging between 0.02 and 1600  $\mu\text{m}$ . Three measurements per sample were carried out. These data were analysed using GRADISTAT version 8.0 (Blott and Pye, 2001) to determine the volumetric percentages of sand (63–1600  $\mu\text{m}$ ), silt (2–63  $\mu\text{m}$ ), and clay (<2  $\mu\text{m}$ ) in each sample.

For total organic carbon and total nitrogen analyses, sediment samples were freeze dried for at least 48 h and then crushed using a mortar and pestle. For each sample, about 100 mg of dry sediments was placed in a silver capsule and acidified with 2 M HCl to remove calcite. The acidified sample was then dried at 50 °C for 24 h and placed in tin capsules for C and N analysis using an elemental analyser (FlashEA, Thermo Fisher Scientific, Waltham, MA, USA).

Bacterial abundance was enumerated after 4',6-diamidino-2-phenylindol staining (Porter and Feig, 1980). Wet sand (1 g) fixed with formaldehyde (final concentration 4%) was diluted with 20 ml of a solution with pyrophosphate (0.1%). Bacteria were detached from sediment by sonication and aliquots were spotted onto slides and stained with 4',6-diamidino-2-phenylindol solution (Schönholzer *et al.*, 2002). The slides were examined at 1000 $\times$  magnification with a microscope fitted for epifluorescence. Bacteria were counted in 30 fields per sample with up to 20 cells per field and were expressed as numbers of bacteria per gramme of dry sediment.

Hydrolytic activity of biofilm was estimated using fluorescein diacetate (FDA) as a substrate for hydrolases. Within 24 h of sampling, FDA was added directly to 1 g of wet sediment in 3 ml of pH 7.6 buffer solution. Incubation was performed at the experimental temperature (15 °C) until a green fluorescein colouration appeared (between 30 and 40 min). The reaction was stopped by freezing the sediment after an addition of 3 ml of acetone following Battin (1997). The optical density of the supernatant was read at

490 nm after filtration on a 0.7- $\mu\text{m}$  glass fiber filter. Results were expressed in micromoles of FDA hydrolysed per gramme of dry sediment per hour ( $\mu\text{mole FDA g}^{-1} \text{h}^{-1}$ ).

Respiration rates of micro-organisms attached to sediment were measured on fresh sediments in a thermostated room at 15 °C using 60-ml respiration chambers. Five grammes of sediment was introduced into respiration chambers filled with filtered water from the Vieux Rhône channel. Control chambers without sediment were also prepared to determine background respiration in the experimental system. An oxygen sensor (UNISENSE, Denmark) coupled with a peristaltic pump was adapted to the respiration chambers to measure the O<sub>2</sub> concentrations in the water every hour for 12 h. The peristaltic pump also mixed water to ensure dissolved oxygen homogeneity in respiration chambers during the incubation. The rate of linear decrease of oxygen concentration with time (from 0 to 12 h) was used to calculate the oxygen respiration for each sediment sample in microgrammes of O<sub>2</sub> consumed per hour. The respiration rates were corrected for respiration measured in control chambers and are reported relative to grammes of dry sediment.

#### Statistical analyses

Cross-correlation analysis was used to compare temperature patterns of surface and hyporheic waters (Box and Jenkins, 1976; Malard *et al.*, 2001). The cross-correlation corresponds to the correlations of the time series of surface water temperature with the time series of hyporheic water temperature, shifted by a particular number of observations performed every 10 min (i.e.  $k = \text{lag}$ ). The cross-correlogram indicates the values of the cross-correlation coefficient ( $r$ ) between surface water and hyporheic water temperature for increasing values of  $k$  ( $x$ -axis shifted forwards) and  $-k$  ( $x$ -axis shifted backwards). Based on the

number of  $k$  corresponding to the highest  $r$  between temperatures of surface and hyporheic waters, we calculated a travel time (in hours) from surface to each hyporheic point in the gravel bar (Foulquier *et al.*, 2009).

For each day of temperature recording, we also calculated the daily thermal amplitude (maximal temperature – minimal temperature) at each point ( $n = 21$  days). The relation between daily thermal amplitudes of surface water and those of hyporheic water was examined using Pearson's correlation coefficient. Damping of daily thermal amplitude with distance within the gravel bar was evaluated in relation with the significance of these correlations in daily thermal amplitude between surface and hyporheic waters.

Two-way ANOVAs were used to evaluate the influence of distance within the gravel bar (1, 15, and 35 m) and sediment structure (fine and coarse sediment structures) on physicochemical, microbial, and faunal variables with distance and sediment structures as main effects. The homoscedasticity and the normality of the data set were verified using Levene's and Shapiro's tests, respectively. Statistical analyses were performed with the Statistica software package (Statsoft Inc., Tulsa, OK, USA). Significance for all statistical tests was accepted at  $\alpha < 0.05$ .

## RESULTS

#### Gravel bar characteristics

The subaerial portion of the bar during the GPR survey had a length of 65 m and a cross-channel dimension of 45 m (Figure 1C). The bar exhibited typical geometry with a high-angle slip face at its tail and a more gently tapered head. The flanks of the bar had a curved, concave-up shape. The presence of the slip face suggested that the bar was actively migrating downstream. Flow was deflected around

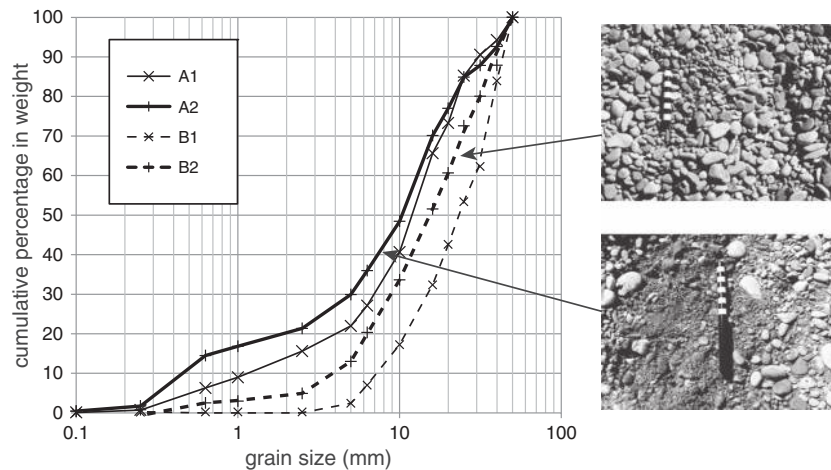


Figure 2. Particle size distribution (cumulative) of the four surface samples obtained from the study site. Photographs illustrate the characteristics of the sediment samples.

the bar at the bar head and wraps around the bar tail, where flow direction was parallel to the slip face during low-flow periods. The bar top was mainly characterized by small dunes (crest height 0.5 m). The observations showed two lithofacies: bimodal gravel (A1 and A2) and open framework gravel (B1 and B2) (Figure 2).

*Radar facies*

Figure 3 showed two radar profiles (GPR2 and GPR5) interpreted with references to specific areas of interest. Interpreted radar facies reflections represented the macroform bounding surfaces because small-scale (centimetre-scale) internal cross stratifications could not be detected with the resolution of the 200-MHz antennae (~0.20 m).

The radar facies R1 is long, sub-horizontal, and continuous. It was easily distinguishable from other

reflectors and was at an elevation of approximately 172.5 m on the 20 GPR profiles. Its location was at the same elevation as the surface of the Vieux Rhône channel, meaning that reflectors indicated the presence of the water table.

The radar facies R2 consisted of sub-horizontal to wavy continuous to discontinuous reflections observed at several depths within the gravel bar. Although some reflections were discontinuous, many of them extended laterally for the entire length of the GPR profiles. In many places, these radar facies reflections serve as bounding for the other radar facies (R3) described in this section. The regular, sub-horizontal to horizontal nature of these layers was a characteristic of sand and gravel deposition by upward stacking. This interpretation of radar facies into lithofacies was confirmed by the grain size analyses of sediment samples A2 at the surface of GPR2 (Figures 1 and 2) and A1 at the surface of GPR1 (Figure 2).

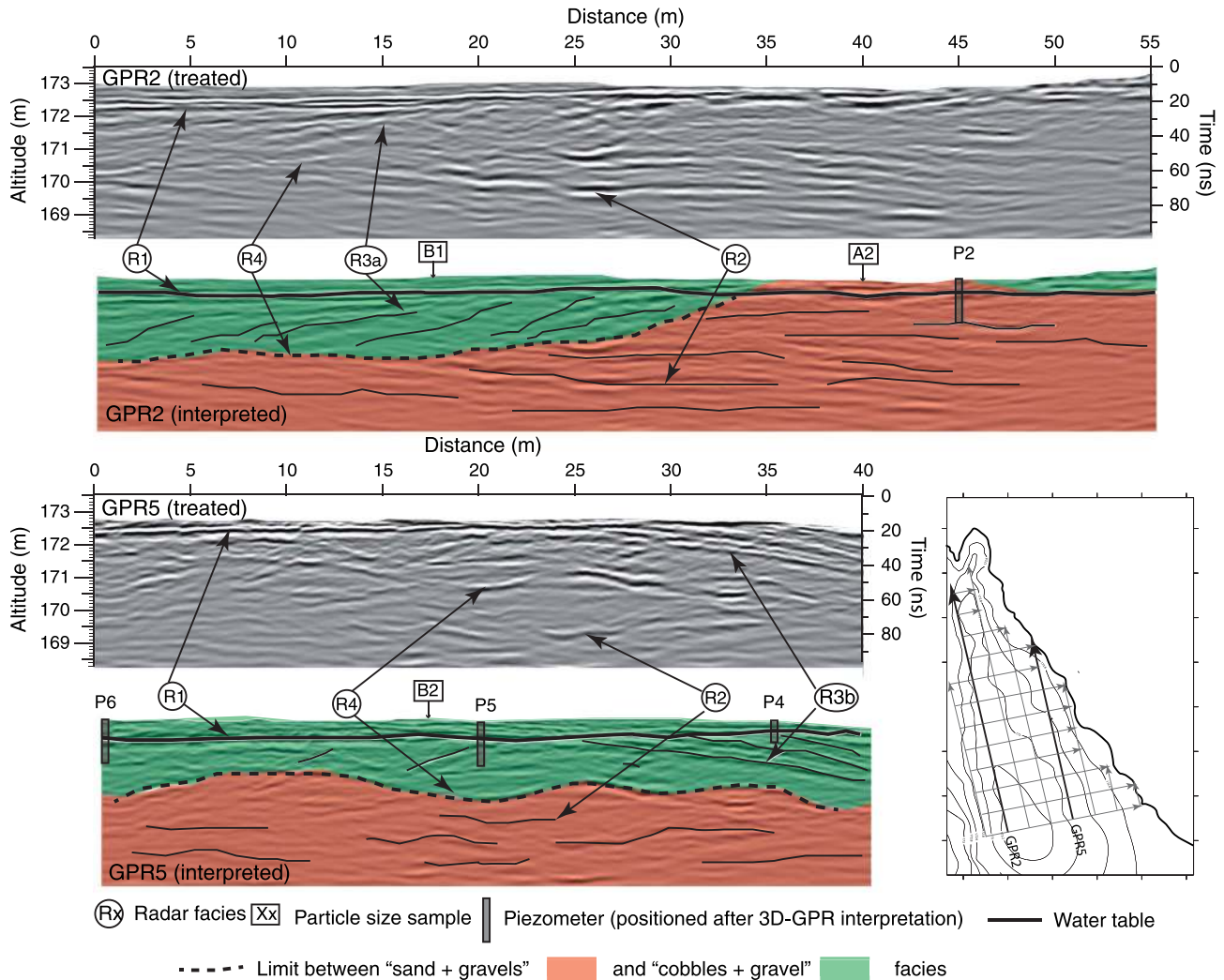


Figure 3. Representative ground-penetrating radar (GPR) profiles and interpretative sketches of the radar facies and major GPR reflection patterns. Location, length, and direction of GPR profile sections are illustrated on the GPR acquisition grid map indicated on the right.

The radar facies R3a and R3b consisted of a set of oblique-parallel reflectors. They were more visible on the east side than on the west side of the gravel bar. These reflectors presented a dip angle of around  $30^\circ$  and were mainly obtained from the transverse profiles (GPR9–GPR18). The occurrence of a relatively steep slip face has been recognized as a characteristic of braided bars (Mumphy *et al.*, 2007). The clear, high-amplitude nature of radar facies reflections was indicative of gravel (high-flow conditions) because the occurrence of sand would have caused, at some degree, signal attenuation. This lithofacies was confirmed by grain size analysis of sediment samples B1 and B2 at the surface of GPR2 and GPR5 (Figures 1 and 2).

The radar facies R4 was a long reflector visible on numerous profiles, which was curvilinear or horizontal. This reflector separated sub-horizontal reflectors R2 from oblique reflectors R3. We presume that this reflector was a limit between the old sediment of the river (former river bed) and the recent sediment deposited during high-flow events.

#### Grid analysis and positioning of piezometers along longitudinal profiles

Based on the determination of the lithofacies on two-dimensional profiles, we obtained a 3D reconstruction of

the facies in the gravel bar (Figure 4) by creating a fence diagram of the GPR profiles. The 3D model was useful in determining the interface between the ‘old’ sediment characterized by cobble/gravel lithofacies and the ‘recent’ sediment characterized by sub-horizontal structure and sand/gravel lithofacies. On the basis of this 3D interpretation, two longitudinal profiles that were sub-parallel to the water flow were selected on the gravel bar (Figure 4): one in the sand and gravel sediments (fine sediment structure, corresponding to A1 and A2 in Figure 2) and the other in the cobbles and gravel (coarse sediment structure corresponding to B1 and B2 in Figure 2). For each longitudinal profile, three positions were determined and equipped with piezometers at increasing distances from the Vieux Rhône channel along the flow path: 1, 15, and 35 m.

#### Hydraulic head and temperature monitoring

Hydraulic head measured in piezometers decreased from the head to the centre of the gravel bar in the two sediment structures (Supplementary Figure S1). Comparable hydraulic gradients were observed in the fine ( $\Delta 35$  cm from 1 to 35 m within the gravel bar) and coarse ( $\Delta 31$  cm from 1 to 35 m within the gravel bar) sediment structures. Hydraulic heads responded quickly to the decrease of water level in

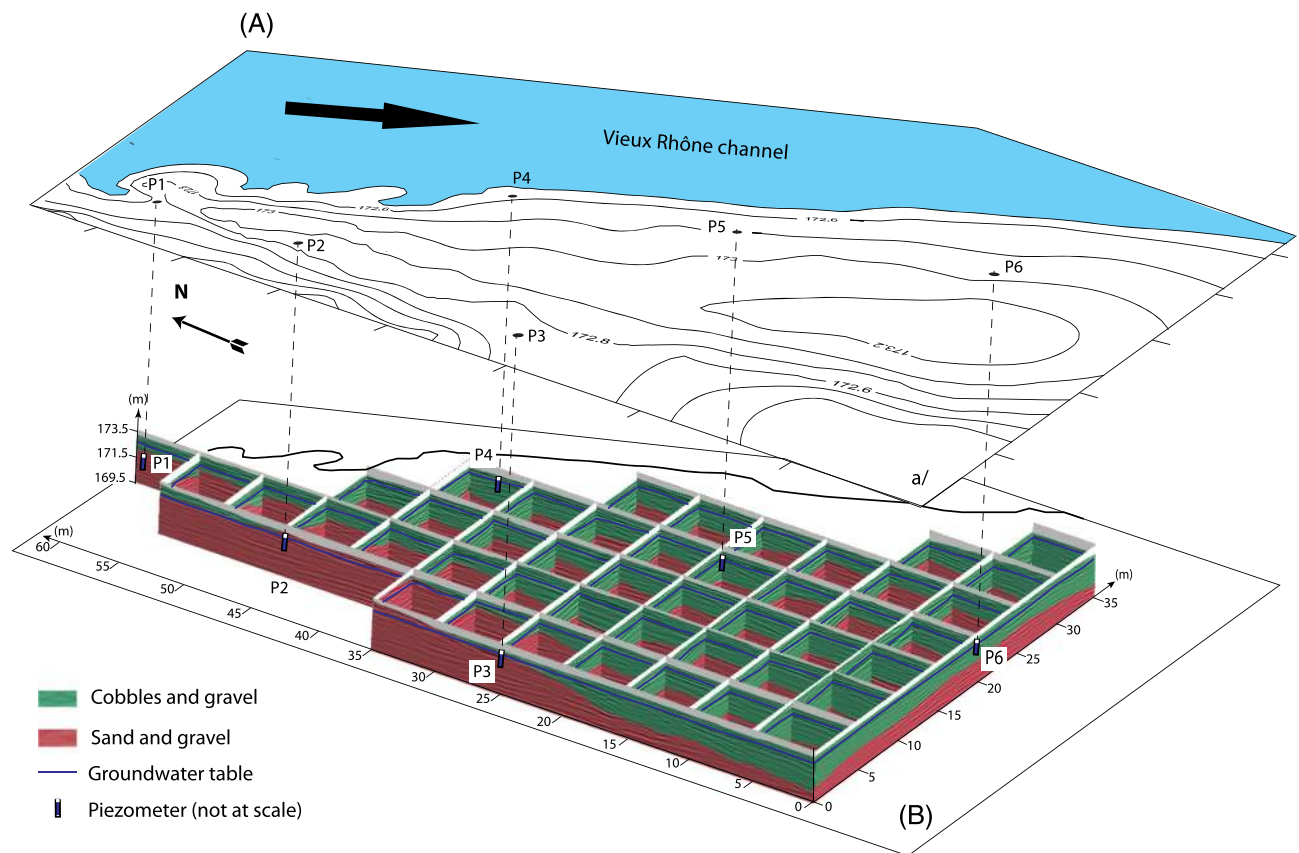


Figure 4. Location of the six piezometers at the surface of the gravel bar (A). Diagram of interpretative sketches of the 20 ground-penetrating radar profiles in the acquisition grid and three-dimensional representation of the two lithofacies with the positions of the piezometers (B).

the Vieux Rhône channel observed on 9 June (Supplementary Figure S1). On the last week of monitoring, we could also note greater variations of water level measured in piezometers located at 15 and 35 m within the gravel bar in comparison with measurements performed in the Vieux Rhône channel and at 1 m within the gravel bar.

Results of the 0.5-h moving-average smoothing of surface water and hyporheic water temperature series recorded from 20 May to 9 June 2011 ( $n=985$ , Figure 5) showed that daily fluctuations of water temperature in the Vieux Rhône channel were rapidly transferred to hyporheic water in the coarse sediment structure. Although a thermal buffering was observed at 15 and 35 m within the gravel bar (Figure 5), daily thermal amplitudes measured in hyporheic water of the coarse sediment structure were significantly correlated with those

of the Vieux Rhône channel (Table I). In contrast, the daily thermal fluctuations monitored in the Vieux Rhône channel were only observed at 1 m within the fine sediment structure, no correlation being obtained between daily thermal amplitudes in surface and hyporheic water for points located at 15 and 35 m within the gravel bar (Table I). The cross-correlations between surface and hyporheic water temperatures indicated that the calculated time of water transport between surface and hyporheic points were more than threefold higher in the fine sediment structure than in the coarse sediment structure for the three monitored positions in the gravel bar (Table I).

#### Water chemistry

Mean water temperature, pH, and concentrations of  $\text{NH}_4^+$  and dissolved organic carbon were not significantly

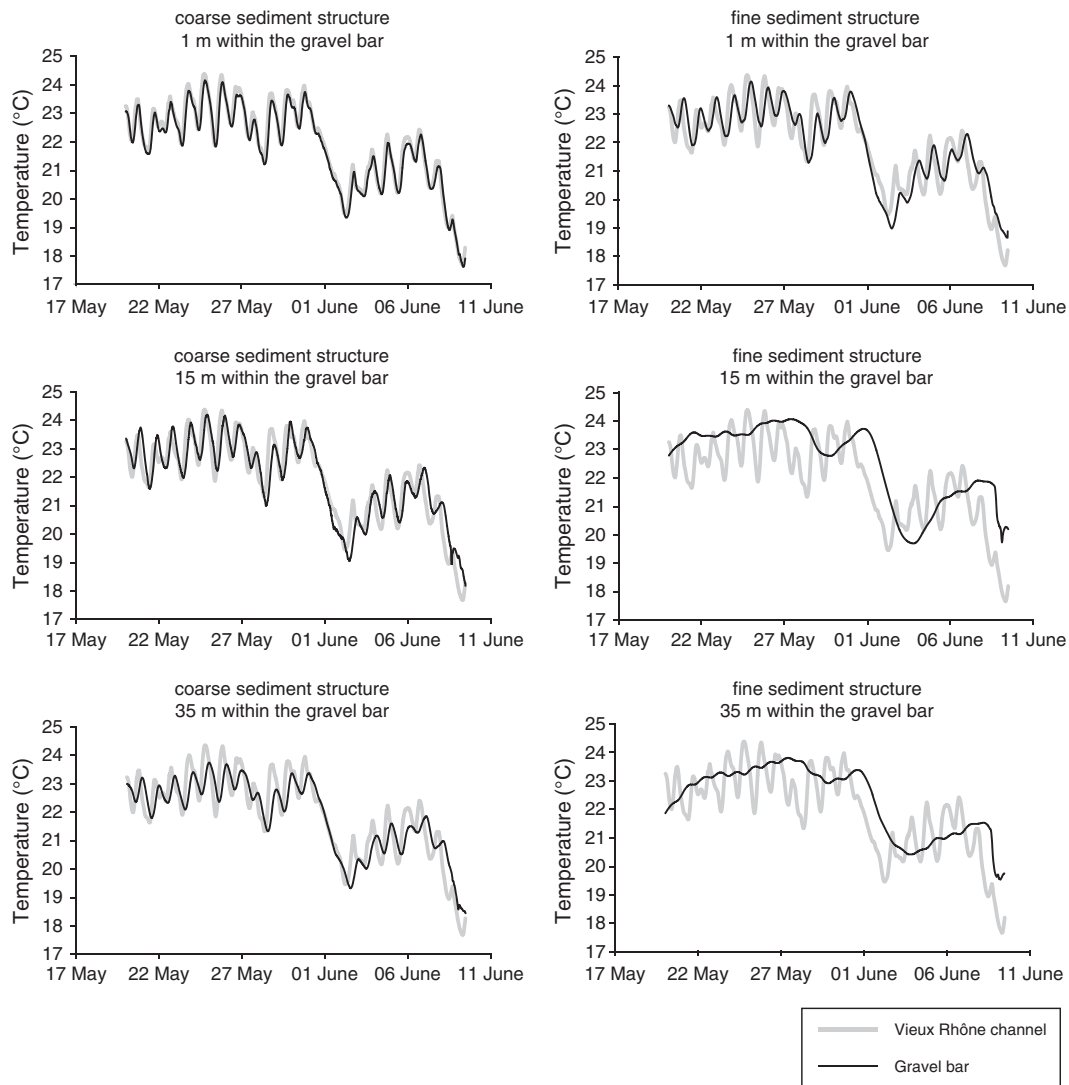


Figure 5. Temperature records for the Vieux Rhône channel (in grey and reported on all panels) and hyporheic habitats (in black) in the two sediment structures and at the three positions within the gravel bar.

Table I. Daily amplitude of water temperature.

Position	Distance from the Vieux Rhône channel (m)	Amplitude (°C)	<i>r</i>	Lag time (hours)
Vieux Rhône channel	0	1.71 (±0.51)	—	—
Coarse sediment structure	1	1.60 (±0.49)	0.956**	1.33
	15	1.63 (±0.37)	0.807**	3.67
	35	1.13 (±0.44)	0.754**	5.33
Fine sediment structure	1	1.38 (±0.32)	0.627*	4.83
	15	0.62 (±0.59)	0.276	16.67
	35	0.48 (±0.52)	0.286	15.00

*r*, Pearson's correlation coefficient between daily amplitude of surface water and hyporheic water temperatures; lag time between surface and hyporheic temperature patterns.

\* $p < 0.01$ , \*\* $p < 0.001$ .

influenced by sediment structure and distance within the gravel bar (Tables II and III). Electrical conductivity and  $\text{NO}_3^-$  concentrations were significantly higher in water collected within the fine sediment structure compared with the coarse sediment structure. Dissolved oxygen and  $\text{PO}_4^{3-}$  concentrations showed the opposite pattern, with significantly lower concentrations in the fine sediment structure compared with the coarse sediment structure. We did not detect significant influence of the distance within the gravel bar on water physicochemistry (Table III) except in interaction with sediment structure effect for dissolved oxygen and phosphate concentrations.

#### Sediment analyses

Analyses of grain size distributions showed that all collected sediment samples were dominated by sand with volumetric fractions ranging between 94.9% and 100%. A small proportion of silt was measured at 1 m in the coarse sediment structure (5.1% in volumetric fraction) and at 1, 15, and 35 m within the fine sediment structure (volumetric fractions: 4.4% at 1 m, 2.2% at 15 m, and 0.5% at 35 m). Both total nitrogen and organic carbon concentrations measured on collected sediments significantly decreased from 1 to 35 m within the gravel bars in the two sediment structures (Figure 6 and Table III). We detected around threefold higher nitrogen and organic carbon concentrations on fine sediments collected at 1 m in the coarse sediment structure compared with those collected in the fine sediment structure at the same distance from the Vieux Rhône channel (Figure 6). This effect was also observed at 15 m within the gravel bar but did not occur at 35 m within the gravel bar (significant interaction effect between sediment structure and distance within the gravel bar, Table III).

#### Microbial analyses

Bacterial abundances varied between  $7 \times 10^9$  cells and  $17 \times 10^9$  cells per gramme of dry sediment (Figure 6). For each sediment structure, the abundances were the highest at

the head (1 m) of the gravel bar (distance effect, Table III). Bacteria were also more numerous on sediments collected in the fine sediment structure compared with sediments sampled from the coarse sediment structure (sediment structure effect, Table III). An opposite pattern was obtained for microbial activities with higher  $\text{O}_2$  consumption and hydrolytic activity on sediments collected in the coarse sediment structure (Figure 6 and Table III). As observed for bacterial abundance, there was a clear decrease of microbial activity between 1 and 15 m along the flow path for the two sediment structures (Table III).

#### Interstitial fauna

We clearly observed a strong decrease in taxa richness and abundance from 1 to 15 m within the gravel bar for the two sediment structures (Figure 6 and distance effect, Table III). Invertebrate assemblages were also more abundant and diverse in samples collected in the coarse sediment structure compared with samples from the fine sediment structure (sediment structure effect, Table III). For instance, it is interesting to note that the common surface-dwelling amphipods of the genus *Gammarus* and the isopod *Asellus aquaticus* were collected in the coarse sediment interstitial habitat but were absent from all hyporheic samples from the fine sediment structure (Table IV). The distribution of the groundwater amphipods of the genus *Niphargus* differed according to the sediment grain size. These animals were collected at 15 and 35 m within the gravel bar in the coarse sediment structure, but only at 1 m in the fine sediment structure.

## DISCUSSION

Our results were in accordance with previous studies (e.g. Naegeli *et al.*, 1996; Brosten *et al.*, 2009), which showed that GPR was an efficient tool to determine the geometry of sediment texture and sediment stratigraphy in gravel bars. Four major radar facies were discerned from

Table II. Physicochemical characteristics of surface water and groundwater collected during the sediment and fauna sampling (on 9 June 2011).

Position	Distance from the Vieux Rhône channel (m)	Temp. (°C)	EC ( $\mu\text{S cm}^{-1}$ )	pH	DO ( $\text{mg l}^{-1}$ )	$\text{NH}_4^+$ ( $\mu\text{g l}^{-1}$ )	$\text{NO}_3^-$ ( $\text{mg l}^{-1}$ )	$\text{PO}_4^{3-}$ ( $\mu\text{g l}^{-1}$ )	DOC ( $\text{mg l}^{-1}$ )
Vieux Rhône channel	0	22-65 ( $\pm 0.21$ )	361 ( $\pm 2$ )	8.0 ( $\pm 0.1$ )	9.35 ( $\pm 0.07$ )	21 ( $\pm 1$ )	4.1 ( $\pm 0.3$ )	27 ( $\pm 1$ )	2.56 ( $\pm 0.04$ )
	1	23-67 ( $\pm 0.21$ )	362 ( $\pm 3$ )	8.2 ( $\pm 0.1$ )	8.88 ( $\pm 0.53$ )	16 ( $\pm 6$ )	4.8 ( $\pm 0.3$ )	23 ( $\pm 13$ )	3.24 ( $\pm 0.33$ )
	15	23-77 ( $\pm 0.64$ )	365 ( $\pm 2$ )	8.0 ( $\pm 0.1$ )	7.61 ( $\pm 0.44$ )	26 ( $\pm 7$ )	5.2 ( $\pm 0.3$ )	30 ( $\pm 4$ )	2.71 ( $\pm 0.17$ )
Coarse sediment structure	35	23-23 ( $\pm 0.31$ )	363 ( $\pm 1$ )	8.0 ( $\pm 0.1$ )	8.21 ( $\pm 0.10$ )	19 ( $\pm 12$ )	4.5 ( $\pm 0.6$ )	37 ( $\pm 1$ )	2.98 ( $\pm 0.97$ )
	1	23-63 ( $\pm 0.59$ )	374 ( $\pm 4$ )	8.0 ( $\pm 0.1$ )	6.04 ( $\pm 0.96$ )	35 ( $\pm 14$ )	5.4 ( $\pm 0.1$ )	30 ( $\pm 1$ )	3.39 ( $\pm 0.15$ )
	15	23-73 ( $\pm 0.15$ )	373 ( $\pm 4$ )	8.1 ( $\pm 0.1$ )	6.73 ( $\pm 0.26$ )	24 ( $\pm 2$ )	5.5 ( $\pm 0.2$ )	18 ( $\pm 7$ )	2.42 ( $\pm 0.28$ )
Fine sediment structure	35	23-53 ( $\pm 0.68$ )	373 ( $\pm 3$ )	8.0 ( $\pm 0.1$ )	6.15 ( $\pm 0.61$ )	25 ( $\pm 1$ )	5.7 ( $\pm 0.1$ )	17 ( $\pm 3$ )	3.60 ( $\pm 0.74$ )

Temp., mean temperature; EC, electric conductivity; DO, dissolved oxygen; DOC, dissolved organic carbon. For all parameters, mean values  $\pm$  standard deviation ( $n = 3$  replicates) are indicated.

GPR profiles (200 MHz). The radar facies R1 with long, sub-horizontal, and continuous reflectors highlighted the water table. The facies R2 with regular, sub-horizontal to horizontal layers was characteristic of sand and gravel deposition by upward stacking, while the facies R3 with oblique-parallel reflectors was characteristic of braided bars and was indicative of the downstream advancement of bars (Regli *et al.*, 2002; Mumphy *et al.*, 2007; Bridge, 2009). This R3 structure was observed in zones where sediment accumulated during high-flow events. Finally, the facies R4 was probably indicative of a limit between the former river bed and more recently deposited sediment. The 3D model obtained allowed us to position piezometers along two longitudinal profiles: one in the ‘old’ sediment characterized by cobble/gravel lithofacies (denoted as ‘coarse sediment structure’) and another in the ‘recent’ sediment characterized by sand/gravel lithofacies (denoted as ‘fine sediment structure’).

This description of sediment structures by GPR associated with hydraulic head measurements was precise enough to determine zones of high and low hydrological flow rates within the hyporheic habitat. Indeed, we could delimitate two longitudinal profiles with distinct hydrological properties and ecological functioning. The coarse sediment structure was characterized by rapid water transport and associated fluxes of dissolved organic matter and nutrients in the hyporheic zone, leading to an enrichment of fine sediments with total organic carbon and total nitrogen. In contrast, the water and nutrient transports were low in the fine sediment structure. As a consequence, the higher flux of organic matter and nutrients in the coarse sediment structure compared with the fine sediment structure was associated with higher microbial activities. Indeed, respiration rates and hydrolytic activities were up to threefold higher in hyporheic sand collected in the coarse sediment structure compared with sand collected in the fine sediment structure.

We can note that these differences in microbial activities between sediment structures were not associated with differences in sediment grain sizes as sand fraction dominated all sediment samples (>94% in volume). Moreover, microbial activities were not tightly linked with bacterial abundances because bacteria were the most numerous per gramme of dry sand in the fine sediment structure. In our experimental conditions, the low quantity of coarse particulate organic matter (leaf litter) did not favour the occurrence of fungi, which could contribute significantly to the measured microbial activities (Romani *et al.*, 2006). Indeed, Findlay *et al.* (2002) reported that most of the microbial biomass associated with sediments and very fine organic matter was due to bacteria rather than fungi. Therefore, the differences of microbial activities measured between the two sediment structures supposed that bacteria were more dormant and/or less active in

Table III. Results of two-way analyses of variance for testing the effects of sediment structure and distance within the gravel bar on physicochemistry, micro-organisms (bacterial abundance and microbial activities) and invertebrate diversity and abundance.

Variable	Sedimentary structure		Distance in the gravel bar		Interaction	
	<i>F</i> (1, 12)	<i>p</i> -value	<i>F</i> (2, 12)	<i>p</i> -value	<i>F</i> (2, 12)	<i>p</i> -value
Temperature	0.11	0.751	0.95	0.413	0.25	0.782
Electric conductivity	49.09	<0.001***	0.22	0.807	0.65	0.537
pH	0.50	0.493	1.50	0.262	3.50	0.063
DO	54.30	<0.001***	0.53	0.603	4.75	0.030*
NH <sub>4</sub> <sup>+</sup>	3.69	0.079	0.30	0.746	2.35	0.138
NO <sub>3</sub> <sup>-</sup>	22.05	<0.001***	1.25	0.321	3.15	0.080
PO <sub>4</sub> <sup>3-</sup>	7.65	0.017*	0.38	0.692	7.07	0.009**
Dissolved organic carbon	0.40	0.539	3.78	0.053	1.08	0.371
Total organic carbon	59.03	<0.001***	28.71	<0.001***	15.81	<0.001***
Total nitrogen	51.48	<0.001***	38.56	<0.001***	17.53	<0.001***
Bacterial abundance	26.87	<0.001***	75.6	<0.001***	7.82	<0.01**
Hydrolytic activity	92.54	<0.001***	57.65	<0.001***	37.40	<0.001***
Respiration rate	48.10	<0.001***	45.12	<0.001***	24.61	<0.001***
Invertebrate diversity	19.10	<0.001***	12.41	<0.005**	0.32	0.733
Invertebrate abundance	15.32	<0.005**	20.15	<0.001***	1.17	0.345

\**p* < 0.05

\*\**p* < 0.01

\*\*\**p* < 0.001

the fine sediment structure than bacteria collected from the coarse sediment structure. We can suggest that the physiological states of bacteria differed in the two sediment structures. The percentage of active bacteria in the hyporheic zone has been shown to vary greatly (2–50% of active bacteria, Fischer *et al.*, 1996; Claret and Fontvieille, 1997) depending on water chemistry and organic matter availability (Fischer *et al.*, 2002; Findlay and Sinsabaugh, 2003; Clinton *et al.*, 2010). In the present study, differences in microbial activities measured between the coarse and fine sediment structures were apparently not related to drastic contrast in the availability of electron acceptors between the two sediment structures. Indeed, mean dissolved oxygen concentrations were higher than 6 mg l<sup>-1</sup> in all hyporheic water samples and did not indicate constraining conditions for micro-organisms in both sediment structures (e.g. Sun *et al.*, 2002). Similarly, variation of mean nitrate concentrations (from 4.1 to 5.7 mg l<sup>-1</sup> of N-NO<sub>3</sub><sup>-</sup>) could not explain the significant differences in microbial activities measured between coarse and fine sediment structures (e.g. Bowen *et al.*, 2009). We can therefore conclude that the threefold differences in microbial activities between sediment samples collected from the coarse and fine sediment structures were more likely related to differences in the availability of organic matter, higher flux of water, and associated dissolved organic matter measured in the coarse sediment structure, probably leading to an increased supply of organic matter available for micro-organisms (Foulquier *et al.*, 2011).

Higher abundances of hyporheic invertebrates in the coarse sediment structure compared with the fine sediment structure suggest that organic matter availability and also

porosity had major influences on invertebrate distribution in the hyporheic zone. The distribution of groundwater organisms in gravel bars is generally linked to groundwater pathways (Dole-Olivier and Marmonier, 1992), but organic matter availability may explain the spatial patterns of groundwater fauna observed in the present study. For instance, the occurrence of *Niphargus* spp. at 15 and 35 m in the coarse sediment structure and at only 1 m in the fine sediment structure might have been due to the occurrence of fine particulate organic matter (FPOM) partially processed during its transport inside the gravel bar. Indeed, FPOM has been recognized as a significant food source for the species *Niphargus rhenorhodanensis* (Navel *et al.*, 2011). Sediment features likely influenced the physical habitat availability of the hyporheic zone for invertebrates. Field studies (Maridet *et al.*, 1992, 1996; Strayer *et al.*, 1997; Olsen and Townsend, 2003) and a laboratory experiment (Navel *et al.*, 2010) showed that pore volume determined the suitability of sediment habitats for invertebrates. Our results were in accordance with this relationship between sediment habitat and invertebrate abundances: the coarse sediment structure allowed the occurrence of large interstitial voids suitable for large crustaceans such as gammarids or asellids, while the fine sediment structure limited the hyporheic habitat availability for large organisms. Therefore, information on the sediment structures obtained by GPR was very efficient to localize biological hotspots in the hyporheic zone although we could not discern the respective influences of organic matter availability and interstitial porosity on fauna distribution in the present study.

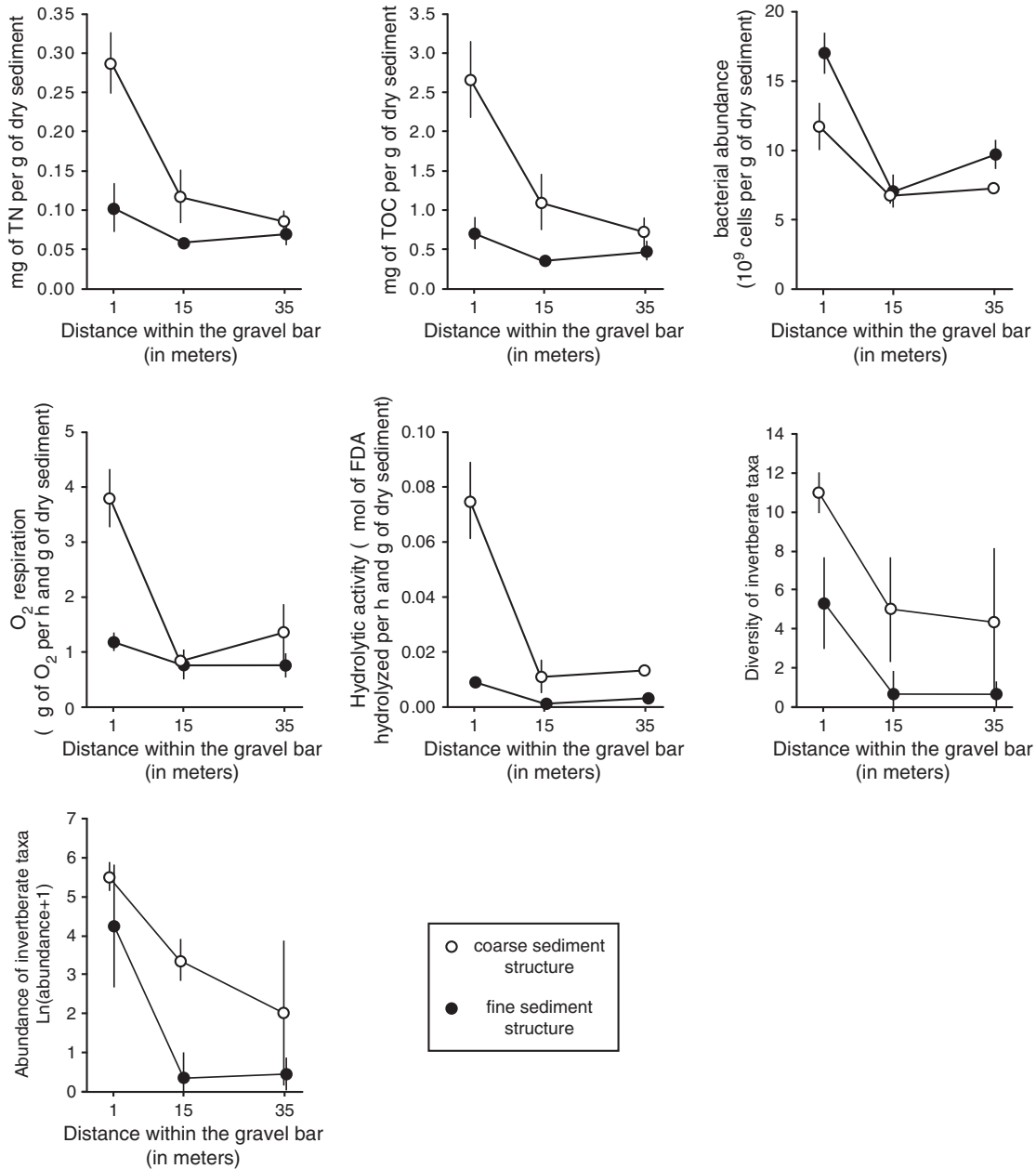


Figure 6. Total nitrogen (TN), total organic carbon, bacterial abundance, microbial activities (oxygen consumption and hydrolytic activity), diversity, and abundance of invertebrates measured in the two sediment structures at three positions within the gravel bar. FDA, fluorescein diacetate.

Several field studies (Danielopol *et al.*, 1992; Mermillod-Blondin *et al.*, 2000; Deforet *et al.*, 2009; Nogaro *et al.*, 2010; Maazouzi *et al.*, 2013) reported high heterogeneity of hyporheic processes at a decametre scale within/between geomorphological units. For instance, Mermillod-Blondin *et al.* (2000) showed that two riffles located 80 m apart in a small French river exhibited functional differences: one riffle acted as a trap for organic matter whereas the other did not. Using an experimental procedure to increase water flow rates, Maazouzi *et al.* (2013) obtained contrasted responses in nutrient dynamics

in the hyporheic zone for two gravel bars located in the same river. In most studies reporting such kind of variability, there is an expected significant influence of local heterogeneities in sediment characteristics (grain size, porosity, and hydraulic conductivity) on groundwater flow paths. The present study highlights the feasibility and usefulness of GPR to test the potential influences of sediment heterogeneities on the location of biological hotspots in the hyporheic zone. The application of GPR would greatly improve our description of the sediment structures in the underground without perturbation by subsurface sediment sampling. Moreover, future applications

Table IV. Abundances of invertebrate taxa (for 101 of collected mixture of water and sediment) collected in the hyporheic zone at three replicated points (1, 2, and 3) per sediment structure (coarse or fine sediment structures) and distance (1, 15, or 35 m) within the gravel bar.

Phylum/class/order	Family	Lowest identification	Coarse sediment structure									Fine sediment structure								
			1 m			15 m			35 m			1 m			15 m			35 m		
			1	2	3	1	2	3	1	2	3	1	2	3	1	2	3	1	2	3
Nematoda/Adenophorea	Mermithoidea	—	15	4	7	2	2	1	1	1	1	29	1							
Oligochaeta	—	—	16	21	24	34	1	3				34	19	10						1
Bivalvia	Sphaeriidae	<i>Pisidium</i> sp.	2	4	2															
Gastropoda	Valvatidae	<i>Valvata</i> sp.	2	4	7			2				25	7	1						
Gastropoda	Hydrobiidae	<i>Potamopyrgus antipodarum</i>	9	2	6															
Copepoda	—	—	200	287	98	4	7	11	1	4	230	27	2	1						
Ostracoda	Candonidae	<i>Pseudocandona zschokkei</i>	3	1	1	1	1													
Cladocera	Chydoridae	<i>Alona guttata</i>		3							4	1								
Cladocera	Chydoridae	<i>Chydorus</i> sp.									1									
Amphipoda	Gammaridae	<i>Gammarus</i> sp.	6	7	15				1											
Amphipoda	Niphargidae	<i>Niphargus</i> sp.				5	9	1	1	40	3									
Isopoda	Asellidae	<i>Asellus aquaticus</i>	4	6																
Arachnida/Acari	—	—						1	8											
Ephemeroptera	Baetidae	—							1											
Plecoptera	Leuctridae	—	2		1															
Coleoptera	Dytiscidae	—	1		3		2													
Coleoptera	Elmidae	<i>Esolus</i> sp.	3	2										1						
Diptera	Chironomidae	<i>Orthocladinae</i> sp.					14													
Diptera	Chironomidae	<i>Chironomini</i> sp.					1													
Diptera	Chironomidae	<i>Tanytarsini</i> sp.					6													
Collembola	—	—	4						5											

of GPR in river systems could include (1) identifying the hyporheic areas acting as main water purification zones in a river and (2) visualizing the preferential water pathways that could act as productive water catchments or vulnerable areas for pollutions.

#### ACKNOWLEDGEMENTS

The authors would like to thank Ivaylo Vassilev, David Goutaland, Laurent Simon, and Felix Vallier for their very efficient assistance during the experiments and Ross Vander-Vorste for his very efficient English editing of the manuscript. This research was carried out on the Research Platform of Crépieux-Charmy (*Plate-forme de recherche de Crépieux-Charmy*) and received financial and technical support from the Greater Lyon Urban Community and Veolia Water. We also thank the reviewers for their comments on the manuscript.

#### REFERENCES

- Battin TJ. 1997. Assessment of fluorescein diacetate hydrolysis as a measure of total esterase activity in natural stream sediment biofilms. *The Science of the Total Environment* **198**(1): 51–60.
- Battin TJ. 2000. Hydrodynamics is a major determinant of streambed biofilm activity: from the sediment to the reach scale. *Limnology and Oceanography* **45**(6): 1308–1319.
- Battin TJ, Kaplan LA, Findlay S, Hopkinson CS, Marti E, Packman AI, Newbold JD, Sabater F. 2008. Biophysical controls on organic carbon fluxes in fluvial networks. *Nature Geoscience* **1**(2): 95–100.
- Bencala KE, Walters RA. 1983. Simulation of solute transport in a mountain pool-and-riffle stream: a transient storage model. *Water Resources Research* **19**(3): 718–724.
- Best JL, Ashworth PJ, Bristow CS, Roden J. 2003. Three dimensional sedimentary architecture of a large, mid-channel sand braid bar, Jamuna River, Bangladesh. *Journal of Sedimentary Research* **73**(4): 516–530.
- Beres M, Green AG, Huggenberger P, Horstmeyer H. 1995. Mapping the architecture of glaciofluvial sediments with three-dimensional georadar. *Geology* **23**(12): 1087–1090.
- Blott SJ, Pye K. 2001. GRADISTAT: a grain size distribution and statistics package for the analysis of unconsolidated sediments. *Earth Surface Processes and Landforms* **26**(11): 1237–1248.
- Bou C, Rouch R. 1967. Un nouveau champ de recherches sur la faune aquatique souterraine. *Comptes Rendus de l'Académie des Sciences Paris* **265**(4): 369–370.
- Bou C. 1974. Les méthodes de récolte dans les eaux souterraines interstitielles. *Annales de Spéléologie* **29**(4): 611–619.
- Boulton AJ, Findlay S, Marmonier P, Stanley EH, Valett HM. 1998. The functional significance of the hyporheic zone in streams and rivers. *Annual Review of Ecology and Systematics* **29**: 59–81.
- Bowen JL, Crump BC, Deegan LA, Hobbie JE. 2009. Increased supply of ambient nitrogen has minimal effect on salt marsh bacterial production. *Limnology and Oceanography* **54**(3): 713–722.
- Box GEP, Jenkins GM. 1976. *Time Series Analysis, Forecasting and Control*. Holden-Day: San Francisco, California, USA.
- Bridge JS, Lunt IA. 2006. Depositional models of braided rivers. In *Braided Rivers: Process, Deposits, Ecology and Management*, Sambrook-Smith GH, Best JL, Bristow CS, Petts GE (eds). Blackwell Publishing: Oxford, UK; 11–49.
- Bridge JS. 2009. Advances in fluvial sedimentology using GPR. In *Ground Penetrating Radar: Theory and Applications*, Jol HM (ed). Elsevier: Amsterdam; 323–359.
- Brosten TR, Bradford JH, McNamara JP, Gooseff MN, Zarnetske JP, Bowden WB, Johnston ME. 2009. Multi-offset GPR methods for hyporheic zone investigations. *Near Surface Geophysics* **7**(4): 247–257.
- Brunke M, Gonser T. 1997. The ecological significance of exchange processes between rivers and groundwater. *Freshwater Biology* **37**(1): 1–33.
- Butturini A, Battin TJ, Sabater F. 2000. Nitrification in stream sediment biofilms: the role of ammonium concentration and DOC quality. *Water Research* **34**(2): 629–639.
- Claret C, Fontvieille D. 1997. Characteristics of biofilm assemblages in two contrasted hydrodynamic and trophic contexts. *Microbial Ecology* **34**(1): 49–57.
- Claret C, Marmonier P, Bravard JP. 1998. Seasonal dynamics of nutrients and biofilms in interstitial habitats in two contrasting riffles in a regulated large river. *Aquatic Sciences* **60**(1): 33–55.
- Clinton SM, Edwards RT, Findlay EG. 2010. Exoenzyme activities as indicators of dissolved organic matter composition in the hyporheic zone of a floodplain river. *Freshwater Biology* **55**(8): 1603–1615.
- Danielopol D, Dreher J, Gunatilaka A, Kaiser M, Niederreiter R, Pospisil P, Creuzé des Châtelliers M, Richter A. 1992. Ecology of organisms living in a hypoxic groundwater environment at Vienna (Austria); methodological questions and preliminary results. In *Proceedings of the First International Conference on Groundwater Ecology*, Simons J, Stanford J (eds). US EPA and AWRA: Tampa FL, USA; 79–90.
- Deforet T, Marmonier P, Rieffel D, Crini N, Giraudoux P, Gilbert D. 2009. Do parafluvial zones have an impact in regulating river pollution? Spatial and temporal dynamics of nutrients, carbon, and bacteria in a large gravel bar of the Doubs River (France). *Hydrobiologia* **623**(1): 235–250.
- Descloux S, Detry T, Philippe M, Marmonier P. 2010. Comparison of different techniques to assess surface and subsurface streambed colmation with fine sediments. *International Review of Hydrobiology* **95**(6): 520–540.
- Dole-Olivier MJ, Marmonier P. 1992. Ecological requirements of stygofauna in an active channel of the Rhône River. *Stygologia* **7**(2): 65–75.
- Fellows CS, Valett HM, Dahm CN. 2001. Whole-stream metabolism in two montane streams: contribution of the hyporheic zone. *Limnology and Oceanography* **46**(3): 523–531.
- Findlay S, Sinsabaugh RL. 2003. Response of hyporheic biofilm metabolism and community structure to nitrogen amendments. *Aquatic Microbial Ecology* **33**(2): 127–136.
- Findlay S, Tank J, Dye S, Valett HM, Mulholland PJ, McDowell WH, Johnson SL, Hamilton SK, Edmonds J, Dodds WK, Bowden WB. 2002. A cross-system comparison of bacterial and fungal biomass in detritus pools of headwater streams. *Microbial Ecology* **43**: 55–66.
- Fischer H, Pusch M, Schwoerbel J. 1996. Spatial distribution and respiration of bacteria in stream-bed sediments. *Archiv für Hydrobiologie* **137**(3): 281–300.
- Fischer H, Wanner SC, Pusch M. 2002. Bacterial abundance and production in river sediments as related to the biochemical composition of particulate organic matter (POM). *Biogeochemistry* **61**(1): 37–55.
- Foulquier A, Malard F, Barraud S, Gibert J. 2009. Thermal influence of urban groundwater recharge from stormwater infiltration basins. *Hydrological Processes* **23**(12): 1701–1713.
- Foulquier A, Mermillod-Blondin F, Malard F, Gibert J. 2011. Response of sediment biofilm to increased dissolved organic carbon supply in groundwater artificially recharged with stormwater. *Journal of Soils and Sediments* **11**: 382–393.
- Gourry JC, Vermeersch F, Garcin M, Giot D. 2003. Contribution of geophysics to the study of alluvial deposits: a case study in the Val d'Avaray area of the river Loire, France. *Journal of Applied Geophysics* **54**(1–2): 35–49.
- Grasshoff K, Ehrhardt M, Kremling K. 1983. *Methods of Seawater Analysis*, 2nd edn. Verlag Chemie: Berlin.
- Heinz J, Kleineidam S, Teutsch G, Aigner T. 2003. Heterogeneity patterns of Quaternary glaciofluvial gravel bodies (SW-Germany): application to hydrogeology. *Sedimentary Geology* **158**(1–2): 1–23.

- Hendricks SP. 1993. Microbial ecology of the hyporheic zone: a perspective integrating hydrology and biology. *Journal of the North American Benthological Society* **12**(1): 70–78.
- Holmes RM, Jones JB, Fisher SG, Grimm NB. 1996. Denitrification in a nitrogen-limited stream ecosystem. *Biogeochemistry* **33**(2): 125–146.
- Huggenberger P, Meier E, Pugin A. 1994. Ground-probing radar as a tool for heterogeneity estimation in gravel deposits: advances in data-processing and facies analysis. *Journal of Applied Geophysics* **31**(1–4): 171–184.
- Jol HM, Bristow CS. 2003. GPR in sediments: advices on data collection basic processing and interpretation, a good practice guide. In *Ground Penetrating in Sediments*, Bristow CS, Jol HM (eds). Geological Society: London, UK, Special Publication 211; 9–27.
- Jones JB, Holmes RM. 1996. Surface–subsurface interactions in stream ecosystems. *Trends in Ecology and Evolution* **11**(6): 239–242.
- Jones JB, Fisher SG, Grimm NB. 1995a. Nitrification in the hyporheic zone of a desert stream ecosystem. *Journal of the North American Benthological Society* **14**(2): 249–258.
- Jones JB, Holmes RM, Fisher SG, Grimm NB, Greene DM. 1995b. Methanogenesis in Arizona, USA dryland streams. *Biogeochemistry* **31**(3): 155–173.
- Jones JB, Fisher SG, Grimm NB. 1995c. Vertical hydrologic exchange and ecosystem metabolism in a Sonoran Desert stream. *Ecology* **76**(3): 942–952.
- Krause S, Hannah DM, Fleckenstein JH, Heppell CM, Kaeser D, Pickup R, Pinay G, Robertson AL, Wood P. 2011. Inter-disciplinary perspectives on processes in the hyporheic zone. *Ecohydrology* **4**(4): 481–499.
- Leclerc RJ, Hickm EJ. 1997. The internal structure of scrolled floodplain deposits based on ground-penetrating radar, North Thompson River, British Columbia. *Geomorphology* **21**(1): 17–38.
- Lefebvre S, Marmonier P, Pinay G. 2004. Stream regulation and nitrogen dynamics in sediment interstices: comparison of natural and straightened sectors of a third order stream. *River Research and Applications* **20**(5): 499–512.
- Lefebvre S, Marmonier P, Pinay G, Bour O, Aquilina L, Baudry J. 2005. Nutrient dynamics in interstitial habitats of low-order rural streams with different bedrock geology (granite versus schist). *Archiv für Hydrobiologie* **164**(2): 169–191.
- Lindhorst S, Betzler C, Hass HC. 2008. The sedimentary architecture of a Holocene barrier spit (Sylt, German Bight): Swash-bar accretion and storm erosion. *Sedimentary Geology* **206**(1–4): 1–16.
- Lunt IA, Bridge JS, Tye RS. 2004. A quantitative three-dimensional depositional model of gravelly braided rivers. *Sedimentology* **51**(5): 377–414.
- Maazouzi C, Claret C, Dole-Olivier MJ, Marmonier P. 2013. Nutrient dynamics in river bed sediments: effects of hydrological disturbances using experimental flow manipulations. *Journal of Soils and Sediments* **13**(1): 207–219.
- Malard F, Mangin A, Uehlinger U, Ward JV. 2001. Thermal heterogeneity in the hyporheic zone of a glacial floodplain. *Canadian Journal of Fisheries and Aquatic Sciences* **58**(7): 1319–1335.
- Maridet L, Wasson JG, Philippe M. 1992. Vertical distribution of fauna in the bed sediment of three running water sites: influence of physical and trophic factors. *Regulated Rivers: Research and Management* **7**(1): 45–55.
- Maridet L, Philippe M, Wasson JG, Mathieu J. 1996. Spatial and temporal distribution of macroinvertebrates and trophic variables within the bed sediment of three streams differing by their morphology and riparian vegetation. *Archiv für Hydrobiologie* **136**(1): 41–64.
- Marmonier P, Delettre Y, Lefebvre S, Guyon J, Boulton AJ. 2004. A simple technique using wooden stakes to estimate vertical patterns of interstitial oxygenation in the beds of rivers. *Archiv für Hydrobiologie* **160**(1): 133–143.
- Mermillod-Blondin F, Creuzé des Chatelliers M, Marmonier P, Dole-Olivier MJ. 2000. Distribution of solutes, microbes and invertebrates in river sediments along a riffle-pool-riffle sequence. *Freshwater Biology* **44**(2): 255–269.
- Miall AD. 1999. *Principles of Sedimentary Basin Analysis*. 3rd, updated and enlarged edn. Springer: Berlin.
- Mitchum RM Jr, Vail PR, Sangree JB. 1977. Stratigraphic interpretation of seismic reflection patterns in depositional sequences. In *Seismic Stratigraphy: Applications to Hydrocarbon Exploration*, Payton CE (ed). The American Association of Petroleum Geologists, Tulsa OK, USA, AAPG Memoir 26; 117–133.
- Mumphy AJ, Jol HM, Kean WF, Isbell JL. 2007. Architecture and sedimentology of an active braid bar in the Wisconsin River based on 3-D ground penetrating radar. In *Stratigraphic Analyses Using GPR*, Baker GS, Jol HM (eds). Geological Society of America: Boulder CO, USA, Special Paper 432; 11–131.
- Naegeli MW, Huggenberger P, Uehlinger U. 1996. Ground penetrating radar for assessing sediment structures in the hyporheic zone of a prealpine river. *Journal of the North American Benthological Society* **15**(3): 353–366.
- Navel S, Mermillod-Blondin F, Montuelle B, Chauvet E, Simon L, Piscart C, Marmonier P. 2010. Interactions between fauna and sediment characteristics control plant matter breakdown in river sediments. *Freshwater Biology* **55**(4): 753–766.
- Navel S, Simon L, Lecuyer C, Fourel F, Mermillod-Blondin F. 2011. The shredding activity of gammarids facilitates the processing of organic matter by the subterranean amphipod *Niphargus rheinorhodanensis*. *Freshwater Biology* **56**(3): 481–490.
- Neal A. 2004. Ground-penetrating radar and its use in sedimentology: principles, problems and progress. *Earth Science Reviews* **66**(3–4): 261–330.
- Nogaro G, Datry T, Mermillod-Blondin F, Descloux S, Montuelle B. 2010. Influence of streambed sediment clogging on microbial processes of the hyporheic zone. *Freshwater Biology* **55**(6): 1288–1302.
- Olsen DA, Townsend CR. 2003. Hyporheic community composition in a gravel-bed stream: influence of vertical hydrological exchange, sediment structure and physicochemistry. *Freshwater Biology* **48**(8): 1363–1378.
- Orghidan T. 1959. Ein neuer lebensraum des unterirdischen wassers: der hyporheische biotop. *Archiv für Hydrobiologie* **55**(3): 392–414.
- Poinsart D, Bravard JP, Caclin MC. 1989. Profil en long et granulométrie du lit des cours d'eau aménagés: l'exemple du canal de Miribel (Haut Rhône). *Revue de Géographie de Lyon* **64**(4): 240–251.
- Poole GC, Stanford JA, Running SW, Frissell CA. 2006. Multiscale geomorphic drivers of groundwater flow paths: subsurface hydrologic dynamics and hyporheic habitat diversity. *Journal of the North American Benthological Society* **25**(2): 288–303.
- Porter KG, Feig YS. 1980. The use of DAPI for identifying and counting aquatic microflora. *Limnology and Oceanography* **25**(5): 943–948.
- Pusch M. 1996. The metabolism of organic matter in the hyporheic zone of a mountain stream, and its spatial distribution. *Hydrobiologia* **323**(2): 107–118.
- Regli C, Huggenberger P, Rauber M. 2002. Interpretation of drill core and georadar data of coarse gravel deposits. *Journal of Hydrology* **255**(1–4): 234–252.
- Romani AM, Fischer H., Mille-Lindblom C, Tranvik LJ. 2006. Interactions of bacteria and fungi on decomposing litter: differential extracellular enzyme activities. *Ecology* **87**(10): 2559–2569.
- Rulík M, Spáčil R. 2004. Extracellular enzyme activity within hyporheic sediments of small lowland stream. *Soil Biology and Biochemistry* **36**(10): 1653–1662.
- Schönholzer F, Hahn D, Zarda B, Zeyer J. 2002. Automated image analysis and in situ hybridization as tools to study bacterial populations in food resources, gut and cast of *Lumbricus terrestris* L. *Journal of Microbiological Methods* **48**(1): 53–68.
- Schrott L, Sass O. 2008. Application of field geophysics in geomorphology: advances and limitations exemplified by case studies. *Geomorphology* **93**(1–2): 55–73.
- Storey RG, Williams DD, Fulthorpe RR. 2004. Nitrogen processing in the hyporheic zone of a pastoral stream. *Biogeochemistry* **69**(3): 285–313.
- Strayer DL, May SE, Nielsen P, Wollheim W, Hausam S. 1997. Oxygen, organic matter, and sediment granulometry as controls on hyporheic animal communities. *Archiv für Hydrobiologie* **140**(1): 131–144.
- Sun MY, Aller RC, Lee C, Wakeham SG. 2002. Effects of oxygen and redox oscillation on degradation of cell-associated lipids in surficial marine sediments. *Geochimica et Cosmochimica Acta* **66**(11): 2003–2012.

- Tonina D, Buffington JM. 2009. Hyporheic exchange in mountain rivers I: mechanics and environmental effects. *Geography Compass* **3**(3): 1063–1086.
- Valett HM, Dahm CN, Campana ME, Morrice JA, Baker MA, Fellows CS. 1997. Hydrologic influences on groundwater–surface water ecotones: heterogeneity in nutrient composition and retention. *Journal of the North American Benthological Society* **16**(1): 239–247.
- Vervier P, Gibert J, Marmonier P, Dole-Olivier MJ. 1992. A perspective on the permeability of the surface freshwater-groundwater ecotone. *Journal of the North American Benthological Society* **11**(1): 93–102.
- Wood PJ, Armitage PD. 1997. Biological effects of fine sediment in the lotic environment. *Environmental Management* **21**(2): 203–217.
- Woodward J, Ashworth PJ, Best JL, Sambrook Smith GH, Simpson CJ. 2003. The use and application of GPR in sandy fluvial environments: methodological considerations. In *Ground Penetrating in Sediments*, Bristow CS, Jol HM (eds). Geological Society: London, UK, Special Publication 211; 127–141.